

# Photolytic Zirconium Benzyl Bond Cleavage and Subsequent Aryl C–F Activation in Zirconium Complexes of Fluorinated Aryl Diamides

Paul E. O'Connor,<sup>†</sup> David J. Berg,<sup>\*,†</sup> and Tosha Barclay<sup>‡</sup>

Department of Chemistry, University of Victoria, P.O. Box 3065,  
Victoria, British Columbia, Canada V8W 3V6, and Chemistry Department,  
North Harris College, 2700 W.W. Thorne Drive, Houston, Texas 77073

Received May 28, 2002

Photolysis of  $\text{Zr}(\text{C}_6\text{F}_5\text{NCH}_2\text{CH}_2\text{OCH}_2)_2(\text{CH}_2\text{Ph})_2$  at 435 nm results in formation of the metalated dimer  $\{\text{Zr}[\text{C}_6\text{F}_4\text{NCH}_2\text{CH}_2\text{OCH}_2\text{CH}_2\text{OCH}_2\text{CH}_2\text{NC}_6\text{F}_5][\text{CH}_2\text{Ph}]\}_2\cdot(\text{C}_7\text{H}_8)_2$  (**1**), the bridging difluoride dimer  $\{\text{Zr}[\text{C}_6\text{F}_5\text{NCH}_2\text{CH}_2\text{OCH}_2\text{CH}_2\text{OCH}_2\text{CH}_2\text{NC}_6\text{F}_5][\text{F}]\}_2[\mu\text{-F}]_2$  (**2**), and bibenzyl. Complex **1** was characterized by NMR spectroscopy ( $^1\text{H}$ ,  $^{19}\text{F}$ ,  $^{13}\text{C}$ ) and X-ray crystallography. In the solid state **1** adopts a pentagonal bipyramidal geometry at each zirconium center with a  $\eta^1$ -benzyl group occupying one of the axial positions. The bridging difluoride **2** was characterized by  $^1\text{H}$  and  $^{19}\text{F}$  NMR spectroscopy. For comparison purposes,  $\text{Zr}(\text{C}_6\text{F}_5\text{NCH}_2\text{CH}_2\text{OCH}_2)_2\text{Me}_2$  (**3**) was synthesized and characterized by NMR spectroscopy and X-ray crystallography. Photolysis of **3** at 435 nm does not result in any reaction.

## Introduction

The photochemical decomposition of alkyl zirconium complexes was first observed more than 30 years ago during the preparation of  $\text{ZrR}_4$  species.<sup>1</sup> This reaction is a serious problem during the preparation of  $\text{Zr}(\text{CH}_2\text{Ph})_4$  in the absence of coordinating solvents, although the exact nature of the decomposition products is still not known. The photochemical formation of low-valent zirconium species, either  $\text{Zr}(\text{III})$  or  $\text{Zr}(\text{II})$ , is well documented,<sup>2,3</sup> although it is unclear in many instances whether the  $\text{Zr}(\text{II})$  oxidation state is formed directly during photolysis<sup>2</sup> or by disproportionation of an unstable trivalent state.<sup>31</sup> The situation is generally com-

plicated by the formation of more than one photoproduct and by rapid thermal reactions, so a definitive understanding of these processes is lacking.<sup>4</sup>

Although C–F bond activation is quite common for electron-rich transition metals,<sup>5</sup> it is far less common with electron-deficient early transition metals despite the exceptional thermodynamic stability of M–F bonds for these elements.<sup>6</sup> In their highest oxidation states, these metals seldom react with fluorocarbons, and many complexes containing fluorinated alkyls and ancillary ligands are known. Perhaps the most significant example of this is the stability of  $\text{B}(\text{C}_6\text{F}_5)_4^-$  and  $\text{B}(\text{p-C}_6\text{H}_4\text{F})_4^-$  counterions in the presence of extremely electron-deficient  $\text{Cp}_2\text{ZrR}^+$  cations, even in the latter case where direct coordination of F to the metal occurs.<sup>7</sup> Most examples of early transition metal C–F activation involve a metal in a reduced oxidation state (e.g.,  $\text{Eu}^{2+}$ ,  $\text{Sm}^{2+}$ ,  $\text{Yb}^{2+}$ ,  $\text{U}^{3+}$ ,  $\text{Ti}^{3+}$ ,  $\text{Zr}^{2+}$ , or  $\text{Zr}^{3+}$ ).<sup>8</sup>

In a previous contribution, we reported the synthesis and structural characterization of several complexes of the type  $\text{Zr}(\text{C}_6\text{F}_5\text{NCH}_2\text{CH}_2\text{OCH}_2)_2(\text{X})(\text{Y})$  ( $\text{X} = \text{Cl}$ ,  $\text{CH}_2\text{Ph}$ ,  $\text{N}(\text{SiMe}_3)_2$ ;  $\text{Y} = \text{Cl}$ ,  $\text{CH}_2\text{Ph}$ ).<sup>9</sup> The alkyl derivatives of this series ( $\text{X}$  and/or  $\text{Y} = \text{CH}_2\text{Ph}$  or  $\text{CH}_2\text{SiMe}_3$ ) show

\* To whom correspondence should be addressed. E-mail: djberg@uvic.ca. Tel: 250-721-7161. Fax: 250-721-7147.

<sup>†</sup> University of Victoria.

<sup>‡</sup> North Harris College.

(1) (a) Zucchini, U.; Albizzati, E.; Giannini, U. *J. Organomet. Chem.* **1971**, *26*, 357. (b) Rausch, M. D.; Boon, W. H.; Alt, H. G. *Ann. N. Y. Acad. Sci.* **1977**, *295*, 103. (c) Ballard, D. G. H.; van Lienden, P. W. *Makromol. Chem.* **1972**, *154*, 177.

(2) (a) Tung, H.; Brubaker, C. H. *Inorg. Chim. Acta* **1981**, *52*, 197. (b) Shibata, K.; Aida, T.; Inoue, S. *Chem. Lett.* **1992**, 1173. (c) Erker, G. *J. Organomet. Chem.* **1977**, *134*, 189. (d) Erker, G.; Wicker, J.; Engel, K.; Krüger, C. *Chem. Ber.* **1982**, *115*, 3300. (e) Erker, G.; Kropp, K.; Atwood, J. L.; Hunter, W. E. *Organometallics* **1983**, *2*, 1555. (f) Erker, G.; Dorf, U. *Angew. Chem., Int. Ed. Engl.* **1983**, *22*, 777.

(3) (a) Samuel, E.; Maillard, P.; Giannotti, C. *J. Organomet. Chem.* **1977**, *142*, 289. (b) Bamford, C. H.; Puddephatt, R. J.; Slater, D. M. *J. Organomet. Chem.* **1978**, *159*, C31. (c) Pankowski, M.; Samuel, E. *J. Organomet. Chem.* **1981**, *221*, C21. (d) Jones, S. B.; Petersen, J. L. *J. Am. Chem. Soc.* **1983**, *105*, 5502. (e) Hudson, A.; Lappert, M. F.; Pichon, R. *J. Chem. Soc., Chem. Commun.* **1983**, 374. (f) Bajgur, C. S.; Jones, S. B.; Petersen, J. L. *Organometallics* **1985**, *4*, 1929. (g) Lappert, M. F.; Raston, C. L. *J. Chem. Soc., Chem. Commun.* **1981**, 173. (h) Czisch, P.; Erker, G.; Korth, H.-G.; Sustmann, R. *Organometallics* **1984**, *3*, 945. (i) Wielstra, Y.; Gambarotta, S.; Meetsma, A.; Spek, A. *Organometallics* **1989**, *8*, 2948. (j) Cacciola, J.; Reddy, K. P.; Petersen, J. L. *Organometallics* **1992**, *11*, 665. (k) Lappert, M. F.; Raston, C. L.; Skelton, B. W.; White, A. H. *J. Chem. Soc., Dalton Trans.* **1997**, 2895. (l) Casty, G. L.; Lugmair, C. G.; Radu, N. S.; Tilley, T. D.; Walzer, J. F.; Zargarian, D. *Organometallics* **1997**, *16*, 8. (m) Dioumaev, V. K.; Harrod, J. F. *Organometallics* **2000**, *19*, 583. (n) Chien, J. C. W.; Wu, J.-C.; Rausch, M. D. *J. Am. Chem. Soc.* **1981**, *103*, 1180. (o) Rausch, M. D.; Boon, W. H.; Alt, H. G. *J. Organomet. Chem.* **1977**, *141*, 299.

(4) Alt, H. G. *Angew. Chem., Int. Ed. Engl.* **1984**, *23*, 766.

(5) Kiplinger, J. L.; Richmond, T. G.; Osterburg, C. E. *Chem. Rev.* **1994**, *94*, 373.

(6) (a) Doherty, N. M.; Hoffman, N. W. *Chem. Rev.* **1991**, *91*, 553. (b) Simões, J. A. M.; Beauchamp, J. L. *Chem. Rev.* **1990**, *90*, 629.

(7) Horton, A. D.; Orpen, A. G. *Organometallics* **1991**, *10*, 3910.

(8)  $\text{Ln}^{2+}$  ( $\text{Ln} = \text{Eu}$ ,  $\text{Sm}$ ,  $\text{Yb}$ ): (a) Deacon, G. B.; MacKinnon, P. I.; Tuong, T. D. *Aust. J. Chem.* **1983**, *36*, 43. (b) Deacon, G. B.; Koplick, A. J.; Raverty, W. D.; Vince, D. G. *J. Organomet. Chem.* **1979**, *182*, 121. (c) Burns, C. J.; Andersen, R. A. *J. Chem. Soc., Chem. Commun.* **1989**, 136. (d) Watson, P. L.; Tulip, T. H.; Williams, I. *Organometallics* **1990**, *9*, 1999.  $\text{U}^{3+}$ : (e) Weydert, M.; Andersen, R. A.; Bergman, R. G. *J. Am. Chem. Soc.* **1993**, *115*, 8837.  $\text{Ti}^{3+}$ : (f) Burk, M. J.; Staley, D. L.; Tumas, W. J. *J. Chem. Soc., Chem. Commun.* **1990**, 809.  $\text{M}^{2+}$  or  $\text{M}^{3+}$  ( $\text{M} = \text{Zr}$ ,  $\text{Ti}$ ): (g) Kiplinger, J. L.; Richmond, T. G. *J. Am. Chem. Soc.* **1996**, *118*, 1805.

(9) O'Connor, P. E.; Morrison, D. J.; Steeves, S.; Burrage, K. Berg, D. *J. Organometallics* **2001**, *20*, 1153.

remarkable thermal stability provided they are protected from ambient light. However, in the presence of light, these compounds darken slowly at room temperature and much more rapidly at elevated temperatures. In the case of the dibenzyl derivative, we observed that a sparingly soluble red crystalline byproduct formed slowly during recrystallization. In this paper, we report the structure of this product and show that it results from the clean photochemical cleavage of a benzyl zirconium bond in  $\text{Zr}(\text{C}_6\text{F}_5\text{NCH}_2\text{CH}_2\text{OCH}_2)_2(\text{CH}_2\text{Ph})_2$  to form a Zr(III) complex followed by intramolecular aryl C–F bond activation to yield a metalated Zr(IV) product.

## Experimental Section

**General Procedures.** All manipulations were carried out under an argon atmosphere, with the rigorous exclusion of oxygen and water, using standard glovebox (Braun MB150-GII) or Schlenk techniques. Tetrahydrofuran (THF), hexane, and toluene were dried by distillation from sodium benzophenone ketyl under argon immediately prior to use.  $\text{Zr}(\text{C}_6\text{F}_5\text{NCH}_2\text{CH}_2\text{OCH}_2)_2\text{Cl}_2$  and  $\text{Zr}(\text{C}_6\text{F}_5\text{NCH}_2\text{CH}_2\text{OCH}_2)_2(\text{CH}_2\text{Ph})_2$  were prepared as previously reported.<sup>9</sup> Tributyltin fluoride was purchased from Aldrich and used as received.

$^1\text{H}$  (360 MHz),  $^{13}\text{C}$  (90.55 MHz), and  $^{19}\text{F}$  (338.86 MHz) NMR spectra were recorded on a Bruker AMX-360 MHz spectrometer. Benzene- $d_6$  was dried over activated 4 Å molecular sieves, and THF- $d_8$  was distilled from sodium benzophenone ketyl and stored over 4 Å molecular sieves prior to use. NMR spectra were recorded using 5 mm tubes fitted with a Teflon valve (Brunfeldt) at room temperature unless otherwise specified.  $^1\text{H}$  and  $^{13}\text{C}$  NMR spectra were referenced to residual solvent resonances.  $^{19}\text{F}$  NMR spectra were referenced to external  $\text{CCl}_3\text{F}$ . Melting points were recorded using a Büchi melting point apparatus and are not corrected. Elemental analyses were performed by Canadian Microanalytical, Delta, B.C.

$\{\text{Zr}[\text{C}_6\text{F}_4\text{NCH}_2\text{CH}_2\text{OCH}_2\text{CH}_2\text{OCH}_2\text{CH}_2\text{NC}_6\text{F}_5][\text{CH}_2\text{Ph}]\}_2 \cdot (\text{C}_7\text{H}_8)_2$  (**1**).  $\text{Zr}(\text{C}_6\text{F}_5\text{NCH}_2\text{CH}_2\text{OCH}_2)_2(\text{CH}_2\text{Ph})_2$  (1.00 g, 1.33 mmol) was weighed into an Erlenmeyer flask in the glovebox and dissolved in 120 mL of toluene. The solution was allowed to stand exposed to ambient light for 11 days, during which time red crystals of **1** deposited from solution. The supernatant was decanted off and allowed to stand for a further 7 days, producing a second crop of **1**. The crystals were washed with toluene and dried under reduced pressure. Total yield: 0.098 g (17%). Further crops of **1** can be obtained, but these are invariably contaminated with increasing amounts of **2**. Mp: 193 °C (dec). NMR (THF- $d_8$ ):  $^1\text{H}$   $\delta$  6.91 (t, 2H, *m*-arylH,  $^3J_{\text{HH}} = 7.7$  Hz), 6.53 (t, 1H, *p*-arylH,  $^3J_{\text{HH}} = 7.3$  Hz), 6.43 (d, 2H, *o*-arylH,  $^3J_{\text{HH}} = 8.2$  Hz), 4.38 (m, 1H), 4.31 (m, 2H), 4.24 (m, 1H), 4.12 (m, 2H), 4.05 (m, 1H), 4.00 (m, 2H), 3.77 (m, 2H), 3.11 (m, 1H), 1.85 (d, 1H,  $\text{CH}_a\text{Ph}$ ,  $^2J_{\text{HH}} = 10.4$  Hz), 1.72 (d, 1H,  $\text{CH}_b\text{Ph}$ ,  $^2J_{\text{HH}} = 10.4$  Hz);  $^{13}\text{C}\{^1\text{H}\}$   $\delta$  151.2 (*quat*-arylC), 146.2 (arylCF,  $^1J_{\text{CF}} = 228$ ), 145.0 (arylCF,  $^1J_{\text{CF}} = 238$ ), 139.4 (arylCF,  $^1J_{\text{CF}} = 256$ ), 136.6 (arylCF,  $^1J_{\text{CF}} = 233$ ), 134.2 (arylCF,  $^1J_{\text{CF}} = 252$ ), 130.0 (*quat*-arylC), 129.3 (arylCF,  $^1J_{\text{CF}} = 228$ ), 129.2 (*quat*-arylC), 128.1 (*m*-arylC), 126.3 (*o*-arylC), 120.3 (*p*-arylC), 77.4 ( $\text{NCH}_2\text{CH}_2\text{O}$ ), 76.9 ( $\text{NCH}_2\text{CH}_2\text{O}$ ), 73.1 ( $\text{OCH}_2\text{CH}_2\text{O}$ ), 71.6 ( $\text{OCH}_2\text{CH}_2\text{O}$ ), 68.0 ( $\text{CH}_2\text{Ph}$ ), 56.4 ( $\text{NCH}_2\text{CH}_2\text{O}$ ), 50.2 ( $\text{NCH}_2\text{CH}_2\text{O}$ );  $^{19}\text{F}\{^1\text{H}\}$   $\delta$  -114.9 (dd, Zr-CCF), -147.1 (d, *o*-arylF,  $^3J_{\text{FF}} = 21$  Hz), -156.2 (t, NCCF), -163.8 (t, *m*-arylCF,  $^3J_{\text{FF}} = 21$  Hz), -165.7 (dd, NCCCF), -167.0 (t, *p*-arylF,  $^3J_{\text{FF}} = 22$  Hz), -170.1 (m, ZrCCCF). Anal. Calcd for  $\text{C}_{57}\text{H}_{46}\text{N}_4\text{O}_4\text{F}_{18}\text{Zr}_2$  (one molecule of toluene per dimer):<sup>10</sup> C, 49.77; H, 3.37; N, 4.07. Found: C, 48.50; H, 3.36; N, 4.09.

(10) Prolonged exposure of this compound to vacuum resulted in partial loss of the toluene of solvation; both  $^1\text{H}$  NMR and elemental analysis showed that only one molecule of toluene per dimer remains after several hours under vacuum.

$\{\text{Zr}[\text{C}_6\text{F}_5\text{NCH}_2\text{CH}_2\text{OCH}_2\text{CH}_2\text{OCH}_2\text{CH}_2\text{NC}_6\text{F}_5][\text{F}]\}_2[\mu\text{-F}]_2$  (**2**). Method 1 (in situ generation during photolysis): A sample of  $\text{Zr}(\text{C}_6\text{F}_5\text{NCH}_2\text{CH}_2\text{OCH}_2)_2(\text{CH}_2\text{Ph})_2$  (0.010 g, 13  $\mu\text{mol}$ ) dissolved in benzene- $d_6$  was placed in a sealable NMR tube under argon. The NMR tube was placed in glass cooling jacket and irradiated with filtered light (435 nm cutoff) from a 150 W incandescent light bulb for 14 h. At the end of this period no trace of starting material was detectable by  $^1\text{H}$  NMR spectroscopy and red crystals of **1** were seen coating the wall of the tube. Compound **2** was characterized in situ by NMR spectroscopy. Larger scale photolysis resulted in precipitation of **2** as a white solid that was very difficult to redissolve. Method 2 (using  $n\text{-Bu}_3\text{SnF}$ ): Solid  $n\text{-Bu}_3\text{SnF}$  (2 equiv) was added to a vigorously stirred solution of  $\text{Zr}(\text{C}_6\text{F}_5\text{NCH}_2\text{CH}_2\text{OCH}_2)_2(\text{CH}_2\text{Ph})_2$  in toluene. After 24 h, solid **2** was filtered away from the toluene supernatant containing  $n\text{-Bu}_3\text{Sn}(\text{CH}_2\text{Ph})$ . The NMR spectrum of **2** generated in this manner was identical to that observed by method 1. Unfortunately, **2** produced by this method was contaminated with unreacted  $n\text{-Bu}_3\text{SnF}$ . NMR (benzene- $d_6$ ):  $^1\text{H}$   $\delta$  3.90 (m, 2H), 3.80 (m, 2H), 3.60 (m, 2H), 3.18 (m, 2H), 2.94 (m, 2H), 2.65 (m, 2H);  $^{19}\text{F}\{^1\text{H}\}$   $\delta$  +109.2 (s, Zr- $F_{\text{term}}$ ), -51.4 (s, Zr- $\mu\text{-F-Zr}$ ), -150.1 (br s, *o*-arylF), -165.8 (t, *p*-arylCF,  $^3J_{\text{FF}} = 20$  Hz), -166.6 (t, *m*-arylF,  $^3J_{\text{FF}} = 21$  Hz). Anal. Calcd for  $\text{C}_{36}\text{H}_{24}\text{N}_4\text{O}_4\text{F}_{24}\text{Zr}_2$ : C, 35.59; H, 1.99; N, 4.61. Found: C, 35.05; H, 1.74; N, 4.55.

$\text{Zr}(\text{C}_6\text{F}_5\text{NCH}_2\text{CH}_2\text{OCH}_2)_2\text{Me}_2$  (**3**). A stirred suspension of  $\text{Zr}[\text{CH}_2\text{OCH}_2\text{CH}_2\text{N}(\text{C}_6\text{F}_5)]_2\text{Cl}_2$  (0.485 g 0.76 mmol) in dry diethyl ether (60 mL) was cooled in a dry ice–acetone bath. MeLi (1.4 M, 1.1 mL, 1.5 mmol) was added via syringe, and the mixture was allowed to stir for 75 min. The Schlenk flask was then transferred to an ice bath and the solvent removed under vacuum. Toluene ( $2 \times 10$  mL) was added to the residue, and the resulting suspension was filtered through Celite. The filtrate was concentrated to ca. 4 mL and cooled at -30 °C to afford **3** as colorless crystals. Repeated recrystallization from toluene afforded crystals suitable for X-ray diffraction. Yield: 0.219 g (48%). Mp: 153 °C dec. NMR (benzene- $d_6$ ):  $^1\text{H}$   $\delta$  3.33 (t, 4H,  $\text{NCH}_2$  or  $\text{OCH}_2\text{CH}_2\text{N}$ ,  $^3J_{\text{HH}} = 5.5$  Hz), 3.11 (t, 4H,  $\text{NCH}_2$  or  $\text{OCH}_2\text{CH}_2\text{N}$ ,  $^3J_{\text{HH}} = 5.5$  Hz), 2.73 (s, 4H,  $\text{OCH}_2\text{CH}_2\text{O}$ ), 0.47 (s, 6H,  $\text{CH}_3$ );  $^{13}\text{C}$   $\delta$  143.1 (d, *o*- or *m*-aryl CF,  $^1J_{\text{CF}} = 234$  Hz), 138.5 (d, *o*- or *m*-aryl CF,  $^1J_{\text{CF}} = 250$  Hz), 133.3 (d, *p*-aryl CF,  $^1J_{\text{CF}} = 271$  Hz), 73.5 (t,  $\text{OCH}_2\text{CH}_2\text{N}$ ,  $^1J_{\text{CH}} = 143$  Hz), 68.9 (t,  $\text{OCH}_2\text{CH}_2\text{O}$ ,  $^1J_{\text{CH}} = 148$  Hz), 52.5 (t,  $\text{NCH}_2$ ,  $^1J_{\text{CH}} = 136$  Hz), 45.2 (q,  $\text{CH}_3$ ,  $^1J_{\text{CH}} = 114$  Hz);  $^{19}\text{F}\{^1\text{H}\}$   $\delta$  -152.0 (d, *o*-arylF,  $^3J_{\text{FF}} = 22$  Hz), -165.5 (t, *m*-arylF,  $^3J_{\text{FF}} = 22$  Hz), -167.3 (t, *p*-arylF,  $^3J_{\text{FF}} = 22$  Hz). UV ( $\text{CH}_2\text{Cl}_2$ ):  $\lambda_{\text{max}}$  277 nm ( $\epsilon$  10 000  $\text{M}^{-1}\text{cm}^{-1}$ ). Anal. Calcd for  $\text{C}_{20}\text{H}_{18}\text{N}_2\text{O}_2\text{F}_{10}\text{Zr}$ : C, 40.06; H, 3.03; N, 4.67. Found: C, 39.71; H, 3.04; N, 4.59.

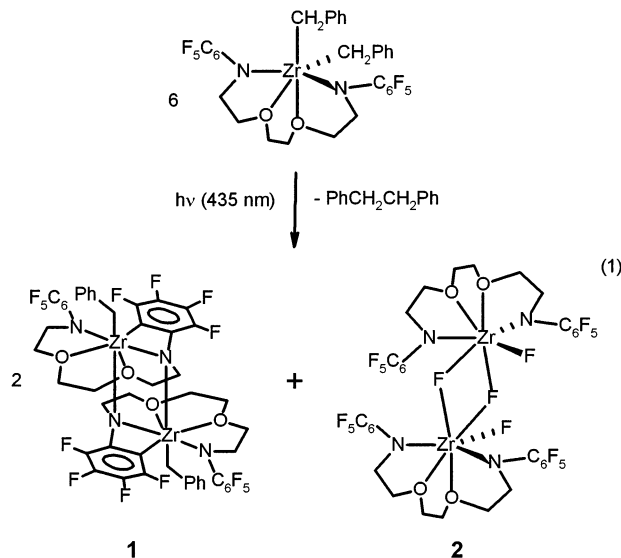
**Photolysis Experiments.** Toluene or benzene- $d_6$  solutions of the samples were irradiated with a 150 W incandescent light bulb. Samples were cooled during irradiation by means of a water jacket. The light was filtered through filters with low-wavelength cutoffs of 375, 435, and 550 nm. Initial experiments showed that only the 435 nm filter afforded clean photoproducts with  $\text{Zr}(\text{C}_6\text{F}_5\text{NCH}_2\text{CH}_2\text{OCH}_2)_2(\text{CH}_2\text{Ph})_2$ . Irradiation using the 375 nm filter resulted in very complex  $^1\text{H}$  NMR spectra consistent with formation of several products. Irradiation at 550 nm did not result in any significant reaction over a period of 28 h. As a control experiment, a solution of  $\text{Zr}(\text{C}_6\text{F}_5\text{NCH}_2\text{CH}_2\text{OCH}_2)_2(\text{CH}_2\text{Ph})_2$  in toluene was wrapped in foil and kept at room temperature for several months; no detectable formation of **1** or **2** was observed, and the starting zirconium complex was recovered unchanged. Irradiation of  $\text{Zr}(\text{C}_6\text{F}_5\text{NCH}_2\text{CH}_2\text{OCH}_2)_2(\text{CH}_2\text{Ph})_2$  in THF- $d_8$  at 435 nm resulted in the formation of bibenzyl and a complex mixture of products that did not contain **1**.

**X-ray Crystallographic Studies.** X-ray quality crystals of **1** deposited directly from the reaction mixture (toluene solution). The crystals were placed in mineral oil under an atmosphere of argon and sealed in a glass capillary. Data were collected on a Siemens Smart 1000 CCD diffractometer

equipped with graphite-monochromated Mo K $\alpha$  radiation ( $\lambda = 0.71073$  Å) at 293 K. Structure solutions were carried out using SHELXS-97,<sup>11</sup> and refinement was done on  $F^2$ . An absorption correction was applied in both cases (abs range: **1** 0.72–1.00; **3** 0.74–1.00). The final Fourier difference maps showed maximum and minimum peaks of  $-0.33/+0.33$  (**1**) and  $-0.50/+0.29$  (**3**) e Å<sup>-3</sup>. Thermal ellipsoid plots were drawn with ORTEP3.<sup>12</sup>

## Results

During a period of several days' exposure to ambient light, a yellow toluene solution of  $\text{Zr}(\text{C}_6\text{F}_5\text{NCH}_2\text{CH}_2\text{OCH}_2)_2(\text{CH}_2\text{Ph})_2$  slowly reacted to form insoluble red crystals of  $\{\text{Zr}[\text{C}_6\text{F}_4\text{NCH}_2\text{CH}_2\text{OCH}_2\text{CH}_2\text{OCH}_2\text{CH}_2\text{NC}_6\text{F}_5][\text{CH}_2\text{Ph}]\}_2 \cdot (\text{C}_7\text{H}_8)_2$  (**1**). At this point the solution contained bibenzyl, identified by NMR spectroscopy,<sup>13</sup> and a zirconium difluoride species **2** discussed in more detail below (eq 1). Control experiments clearly showed that the reaction was photochemical in nature, as toluene solutions of  $\text{Zr}(\text{C}_6\text{F}_5\text{NCH}_2\text{CH}_2\text{OCH}_2)_2(\text{CH}_2\text{Ph})_2$  wrapped in foil were recovered unchanged after several months at room temperature. In addition, the reaction was found to proceed to completion in 14 h when photolysis was carried out using a 150 W incandescent light source masked with a 435 nm filter. Photolysis using a longer wavelength filter (550 nm) resulted in no detectable reaction over a period of days. Photolysis at shorter wavelengths (375 nm) produced a complex mixture of products. This strong wavelength dependence confirms the photochemical nature of the reaction in eq 1.



The red crystals of **1** are very insoluble in hydrocarbon solvents and do not recrystallize well from ethereal solvents. Fortunately, the crystals obtained from the reaction mixture were of sufficient quality to allow us to establish the structure of this compound by X-ray

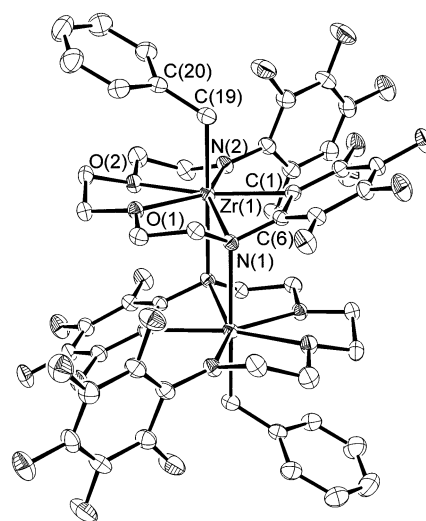


**Figure 1.** ORTEP3 drawing<sup>12</sup> (thermal ellipsoids at 30% probability) of **1**. The toluene of solvation is omitted for clarity.

**Table 1.** Summary of Crystallographic Data

	<b>1</b>	<b>3</b>
formula	$\text{C}_{64}\text{H}_{54}\text{N}_4\text{O}_4\text{F}_{18}\text{Zr}_2$	$\text{C}_{20}\text{H}_{18}\text{N}_2\text{O}_2\text{F}_{10}\text{Zr}$
fw	1467.55	599.58
cryst syst	triclinic	triclinic
space group	$P\bar{1}$ (No. 2)	$P\bar{1}$ (No. 2)
$a$ (Å)	8.9913(11)	8.8830(18)
$b$ (Å)	11.0332(14)	10.415(2)
$c$ (Å)	15.2867(19)	13.156(3)
$\alpha$ (deg)	82.974(2)	83.147(4)
$\beta$ (deg)	79.912(2)	74.269(4)
$\gamma$ (deg)	87.465(2)	82.043(4)
$V$ (Å <sup>3</sup> )	1481.4(3)	1156.0(4)
$Z$	1	2
$\rho$ (calcd) (g cm <sup>-3</sup> )	1.64	1.72
$\mu$ (mm <sup>-1</sup> )	0.46	0.58
$\lambda$ (Å)	Mo K $\alpha$ , 0.7107	Mo K $\alpha$ , 0.7107
$T$ (K)	293	293
$2\theta_{\text{max}}$ (deg)	50	50
no. obsd rflns	11 259	6268
no. of unique rflns	5201	4065
$F_{000}$	740	596
$R^a$	0.031	0.037
$R_w^b$	0.067	0.072

$$^a R = \sum(|F_o| - |F_c|)/\sum|F_o|. \quad ^b R_w = [\sum w(|F_o| - |F_c|)^2/\sum w|F_o|^2]^{1/2}.$$

crystallography. The ORTEP3 drawing of **1** (Figure 1) shows a centrosymmetric dimer containing amido nitrogen bridges between the two zirconium centers. Data collection parameters are given in Table 1, and selected bond distances and angles are listed in Table 2. Each half of the dimer consists of a metalated  $\text{C}_6\text{F}_4\text{NCH}_2\text{CH}_2\text{OCH}_2\text{CH}_2\text{OCH}_2\text{CH}_2\text{NC}_6\text{F}_5$  ligand bound to the metal by two anionic amido nitrogens, two neutral ether oxygens, and the anionic *ortho* carbon of the metalated  $\text{C}_6\text{F}_4$  ring. The five bonded atoms and the zirconium atom lie approximately in a plane (maximum deviations: N(1) +0.35 Å and O(1) -0.26 Å). This leads to a pentagonal bipyramidal geometry at the metal center when the axial benzyl group and bridging amido nitrogen from the other ligand are included.<sup>14</sup> The bridging amido group of each ligand is that which is bonded to the metalated  $\text{C}_6\text{F}_4$  ring. Presumably this amido nitrogen bridges because metalation constrains the  $\text{C}_6\text{F}_4$  ring to be nearly coplanar with the pentagonal plane (dihedral angle 24°), thus minimizing steric repulsions incurred by face-to-face dimerization of monomeric units. In

(11) Sheldrick, G. *SHELX-97: Programs for Crystal Structure Determination*; University of Göttingen, Germany, 1997.

(12) Farrugia, L. J. ORTEP3 for Windows. *J. Appl. Crystallogr.* **1997**, *30*, 565.

(13) Bibenzyl was identified by its characteristic <sup>1</sup>H and <sup>13</sup>C NMR CH<sub>2</sub> resonances: <sup>1</sup>H NMR (CDCl<sub>3</sub>)  $\delta$  2.90; <sup>13</sup>C NMR 37.9 (t) ppm. Literature: Pouchert, C. J.; Behnke, J. *Aldrich Library of <sup>13</sup>C and <sup>1</sup>H FT NMR Spectra, Edition 1*; Aldrich Chemical Co.: 1993; Vol. 2, p 8A.



**Table 2.** Selected Bond Distances (Å) and Angles (deg) for **1**

Bond Distances			
Zr(1)–N(1)	2.308(2)	Zr(1)–N(2)	2.163(2)
Zr(1)–N(1)'	2.401(2)	Zr(1)–O(1)	2.286(2)
Zr(1)–O(2)	2.285(2)	Zr(1)–C(1)	2.326(3)
Zr(1)–C(19)	2.314(3)		
Bond Angles			
N(1)–Zr(1)–N(2)	150.29(8)	N(1)–Zr(1)–N(1)'	74.85(7)
N(1)–Zr(1)–O(1)	69.70(7)	N(1)–Zr(1)–O(2)	133.18(7)
N(1)–Zr(1)–C(1)	61.51(8)	N(1)–Zr(1)–C(19)	91.93(9)
N(2)–Zr(1)–N(1)'	94.10(7)	N(2)–Zr(1)–O(1)	138.92(7)
N(2)–Zr(1)–O(2)	72.40(7)	N(2)–Zr(1)–C(1)	93.08(9)
N(2)–Zr(1)–C(19)	99.30(9)	O(1)–Zr(1)–N(1)'	90.02(6)
O(1)–Zr(1)–O(2)	66.89(6)	O(1)–Zr(1)–C(1)	127.20(8)
O(1)–Zr(1)–C(19)	81.81(8)	O(2)–Zr(1)–N(1)'	88.34(7)
O(2)–Zr(1)–C(1)	165.23(8)	O(2)–Zr(1)–C(19)	98.44(9)
C(1)–Zr(1)–N(1)'	95.56(8)	C(1)–Zr(1)–C(19)	80.89(9)
C(19)–Zr(1)–N(1)'	166.28(8)	Zr(1)–N(1)–Zr(1)'	105.15(7)
Zr(1)–N(1)–C(6)	90.8(2)	Zr(1)–N(1)–C(7)	111.2(2)
Zr(1)–N(1)–C(6)	114.8(2)	(2)Zr(1)–N(1)–C(7)	116.3(2)
Zr(1)–N(2)–C(12)	115.5(2)	(2)Zr(1)–N(2)–C(13)	134.1(2)
Zr(1)–C(1)–C(6)	90.5(2)	Zr(1)–C(19)–C(20)	118.5(2)
N(1)–C(6)–C(1)	113.8(2)	C(6)–N(1)–C(7)	115.0(2)
C(12)–N(2)–C(13)	110.1(2)		

contrast, the C<sub>6</sub>F<sub>5</sub> ring lies nearly perpendicular (dihedral angle 98°) to the pentagonal plane, and this would clearly hinder dimerization through the amido nitrogen bonded to it.

The geometry at the two amido nitrogens differs markedly. The bridging amido nitrogen is pyramidal, with bond angles ranging from 105.15(7)° (Zr(1)–N(1)–Zr(1)') to 116.27(15)° (C(7)–N(1)–Zr(1)'); as might be expected, the angle involving the aryl carbon of the metalated ring is significantly distorted from normal tetrahedral values (Zr(1)–N(1)–C(6) 90.8(2)°). The other amido nitrogen displays the planar coordination geometry (sum of angles about N(2) = 359.7°) commonly found in complexes of early transition metals. Consistent with the difference in geometry, the bridging amido nitrogen has a longer Zr–N distance than the nonbridging amido nitrogen (Zr(1)–N(1) 2.308(2) Å; Zr(1)–N(2) 2.163(2) Å). The terminal Zr–N bond length found in this structure is significantly longer than those observed in Zr{[CH<sub>2</sub>OCH<sub>2</sub>CH<sub>2</sub>N(C<sub>6</sub>F<sub>5</sub>)<sub>2</sub>]<sub>2</sub>}[N(SiMe<sub>3</sub>)<sub>2</sub>]Cl (2.102(5), 2.131(5), and 2.100(5) Å),<sup>9</sup> Zr{[CH<sub>2</sub>OCH<sub>2</sub>CH<sub>2</sub>N(C<sub>6</sub>F<sub>5</sub>)<sub>2</sub>]<sub>2</sub>}[CH<sub>2</sub>Ph]Cl (2.076(9) and 2.076(10) Å),<sup>9</sup> or zirconium complexes containing a terminal dimethylamido group (average Zr–N 2.055 Å)<sup>15a–f</sup> and alkyl aryl amides (av = 2.08 Å).<sup>15g–l</sup> There is also significant asymmetry in the bridging Zr–N distances (Zr(1)–N(1) 2.308(2) Å,

Zr(1)–N(1) 2.401(3) Å). Asymmetry in Zr–N bond lengths is normally observed in bridging dimethylamido complexes, although the difference observed in **1** is considerably less than that usually observed ( $\Delta = 0.09$  Å for **1** compared with  $\Delta = 0.18$  Å for Zr<sub>2</sub>( $\mu$ -NMe<sub>2</sub>)<sub>15a–f</sub>). This discrepancy is entirely accounted for by a lengthening of the "short" Zr–N distance within the pentagonal plane (i.e., between each Zr and the bridging amido nitrogen of its own chelating ligand) by ca. 0.09 Å in comparison to the distance predicted from bridging dimethylamido zirconium complexes.<sup>15a–f</sup> In contrast the "long" bridging Zr(1)–N(1) distance is very similar to that observed in bridging dimethylamido complexes (av 2.396 Å).<sup>15a–f</sup> The observed trends in bond lengths are consistent with significant crowding within the pentagonal plane but less crowding in the axial positions.

The benzyl group in **1** is bonded  $\eta^1$  to the zirconium center (Zr(1)–C(19)–C(20) 118.52(18)°). The benzyl Zr–C bond distance (Zr(1)–C(19) 2.314(3) Å) compares well with the distance observed in Zr{[CH<sub>2</sub>OCH<sub>2</sub>CH<sub>2</sub>N(C<sub>6</sub>F<sub>5</sub>)<sub>2</sub>]<sub>2</sub>}[CH<sub>2</sub>Ph]Cl (2.292(11) Å)<sup>9</sup> and those reported in the literature for a wide range of benzyl zirconium complexes.<sup>16</sup> The Zr–C bond distance to the metalated aryl ring (Zr(1)–C(1) 2.326(3) Å) is well within the range normally observed for Zr–phenyl bonds,<sup>17</sup> although it is significantly longer than that found in the only other structurally characterized zirconium complex containing a four-membered ZrNC<sub>2</sub> ring (2.289(4) Å).<sup>16d</sup> This may also reflect steric crowding within the pentagonal plane.

Complex **1** dissolves sufficiently in THF-*d*<sub>8</sub> to obtain NMR spectra. The <sup>1</sup>H NMR spectrum shows a low-symmetry environment where the inequivalent ligand backbone protons appear as a series of overlapping multiplets between 3.1 and 4.4 ppm. The benzylic protons are also inequivalent and appear as AB doublets at 1.85 and 1.72 ppm. As expected, all six carbons of

(15) Zirconium complexes containing both bridging and terminal dimethylamides: (a) Daniele, S.; Hitchcock, P. B.; Lappert, M. F.; Merle, P. G. *J. Chem. Soc., Dalton Trans.* **2001**, 13. (b) Chisholm, M. H.; Hammond, C. E.; Huffman, J. C. *Polyhedron* **1988**, 7, 2515. (c) Liu, X.; Wu, Z.; Peng, Z.; Wu, Y. Xue, Z. *J. Am. Chem. Soc.* **1999**, 121, 5350. (d) Kempe, R.; Hillenbrand, G.; Spannenberg, A. Z. *Kristallogr.-New Cryst. Struct.* **1997**, 212, 490. (e) Wu, Z.; Diminnie, J. B.; Xue, Z. *Inorg. Chem.* **1998**, 37, 2570. (f) Petz, W.; Weller, F.; Avtomonov, E. V. *J. Organomet. Chem.* **2000**, 598, 403. For some representative zirconium complexes containing terminal alkyl aryl amides see: (g) Zhang, X.; Zhu, Q.; Guzei, I. A.; Jordan, R. F. *J. Am. Chem. Soc.* **2000**, 122, 8093. (h) Mehrkhodavandi, P.; Bonitatebus, P. J.; Schrock, R. R. *J. Am. Chem. Soc.* **2000**, 122, 7841. (i) McMullen, A. K.; Rothwell, I. P.; Huffman, J. C. *J. Am. Chem. Soc.* **1985**, 107, 1072. (j) Polamo, M.; Mutikainen, I.; Leskela, M. Z. *Kristallogr.* **1996**, 211, 641. (k) Kasani, A.; Gamarotta, S.; Bensimon, C. *Can. J. Chem.* **1997**, 75, 1494. (l) Scollard, J. D.; McConville, D. H.; Vittal, J. J. *Organometallics* **1995**, 14, 5478.

(16) For a representative sample of structurally characterized zirconium benzyl complexes containing multidentate ancillary ligands please see: (a) Tshura, E. Y.; Goldberg, I.; Kol, M.; Weitman, H.; Goldschmidt, Z. *J. Chem. Soc., Chem. Commun.* **2000**, 379. (b) Guerin, F.; McConville, D. H.; Vittal, J. J.; Yap, G. A. P. *Organometallics* **1998**, 17, 5172. (c) Ziniuk, Z.; Goldberg, I.; Kol, M. *Inorg. Chem. Commun.* **1999**, 2, 549. (d) Qian, B.; Scanlon, W. J.; Smith, M. R.; Motry, D. H. *Organometallics* **1999**, 18, 1693. (e) Shao, P.; Gendron, R. A. L.; Berg, D. J.; Bushnell, G. W. *Organometallics* **2000**, 19, 509. (f) Morton, C.; Munslow, I. J.; Sanders, C. J.; Alcock, N. W.; Scott, P. *Organometallics* **1999**, 18, 4608. (g) Giesbrecht, G. R.; Shafir, A.; Arnold, J. J. *Chem. Soc., Chem. Commun.* **2000**, 2135. (h) Morton, C.; Gillespie, K. M.; Sanders, C. J.; Scott, P. *J. Organomet. Chem.* **2000**, 606, 141. (i) Aizenberg, M.; Turculet, L.; Davis, W. M.; Schattenmann, F.; Schrock, R. R. *Organometallics* **1998**, 17, 4795. (j) Schrock, R. R.; Seidel, S. W.; Schrodi, Y.; Davis, W. M. *Organometallics* **1999**, 18, 428. (k) Graf, D. D.; Schrock, R. R.; Davis, W. M.; Stumpf, R. *Organometallics* **1999**, 18, 843. (l) Schrock, R. R.; Baumann, R.; Reid, S. M.; Goodman, L. T.; Stumpf, R.; Davis, W. M. *Organometallics* **1999**, 18, 3649.

(14) Structurally characterized seven-coordinate zirconium complexes adopting a pentagonal bipyramidal geometry include zirconium fluoride derivatives<sup>14a–h</sup> and complexes containing polydentate alkoxy- and aminoethers.<sup>14i–l</sup> (a) Bukvetskii, B. V.; Gerasimenko, A. V.; Davidovich, R. L.; Medkov, M. A. *Koord. Khim.* **1985**, 11, 77. (b) Nelson, M. J.; Girolami, G. S. *J. Organomet. Chem.* **1999**, 585, 275. (c) Bukvetskii, B. V.; Gerasimenko, A. V.; Kondratyuk, I. P.; Davidovich, R. L.; Medkov, M. A. *Koord. Khim.* **1987**, 13, 77. (d) Gao, Y.; Guery, J.; Jacobini, C. *Acta Crystallogr. C* **1993**, 49, 963. (e) Alcock, N. W.; Errington, W.; Golby, S. L.; Patterson, S. M. C.; Wallbridge, M. G. H. *Acta Crystallogr. C* **1994**, 50, 226. (f) Il'in, E. G.; Roesky, H. W.; Aleksandrov, G. G.; Kovalev, V. V.; Sergeev, A. V.; Yagodin, V. G.; Sergienko, V. S.; Shchelokov, R. N.; Buslaev, Y. A. *Dokl. Akad. Nauk SSSR* **1997**, 355, 349. (g) Errington, W.; Ismail, M. A. *Acta Crystallogr. C* **1994**, 50, 1540. (h) Prinz, H.; Bott, S. G.; Atwood, J. L. *J. Am. Chem. Soc.* **1986**, 108, 2113. (i) Alvanipour, A.; Atwood, J. L.; Bott, S. G.; Junk, P. C.; Kynast, U. H.; Prinz, H. *J. Chem. Soc., Dalton Trans.* **1998**, 1223. (j) Polamo, M.; Leskela, M. *J. Chem. Soc., Dalton Trans.* **1996**, 4345. (k) Male, N. A. H.; Thornton-Pett, M.; Bochmann, M. *J. Chem. Soc., Dalton Trans.* **1997**, 2487. (l) Schweder, B.; Walther, D.; Dohler, T.; Klobes, O.; Gorus, H. *J. Prakt. Chem.-Chem.-Zeitung* **1999**, 341, 736.

the ligand backbone are inequivalent in the  $^{13}\text{C}$  NMR spectrum and the benzylic carbon appears at 68.0 ppm (observable in the DEPT spectrum). The  $^{19}\text{F}$  NMR shows seven inequivalent fluorine resonances. Interestingly, the resonance due to the fluorine *ortho* to the metalated carbon appears far downfield ( $\delta$  -114.9 ppm) of the other resonances ( $\delta$  -147 to -171 ppm). It is noteworthy that this fluorine is positioned over the face of the  $\text{C}_6\text{F}_5$  ring of the same ligand in the crystal structure (F(1)–C distances (Å): C(13) 3.089(4), C(14) 3.548(4), C(15) 3.782(4), C(16) 3.546(4), C(17) 3.066(4), C(18) 2.819(4)). This may provide some evidence that the solid state structure of **1** is maintained in solution, although it is possible that the same relative positioning of this fluorine with respect to the  $\text{C}_6\text{F}_5$  ring could be maintained even if the dimer were to fragment into monomers (with THF occupying the coordination site held by the bridging amido group, for example).

The observation that bibenzyl was produced along with **1** and that no benzyl fluoride was detectable by NMR spectroscopy strongly suggested formation of a zirconium fluoride species. When the photolysis reaction was repeated in benzene- $d_6$  solution in an NMR tube, a single soluble zirconium product (**2**) containing aryl-diamide ligand resonances was observed (**1** deposits as benzene-insoluble crystals on the walls of the tube). This product also proved to be sparingly soluble in hydrocarbons, which prevented adequate characterization by  $^{13}\text{C}$  NMR spectroscopy; however, we were able to obtain  $^1\text{H}$  and  $^{19}\text{F}$  NMR data. While the  $^1\text{H}$  spectrum of **2** simply contains six multiplets for the ligand backbone, the  $^{19}\text{F}$  spectrum is far more informative. In addition to the multiplets due to the  $\text{C}_6\text{F}_5$  ring between -150 and -167 ppm, two new singlets are observed at +109.2 and -51.4 ppm. The downfield resonance is well outside the range found for fluorinated aryl groups<sup>18</sup> but is consistent with a terminal Zr–F.<sup>19</sup> The resonance at -51.4 ppm is also too far downfield to arise from an aryl-CF group, but it agrees quite well with the chemical shifts normally observed for bridging fluorides of the type Zr–F–Zr.<sup>20</sup> Although these data are not sufficient to unambiguously assign the structure of **2**, they are consistent with the structure shown in eq 1. Complex **2** slowly precipitates from solution as a pale yellow glassy solid that is often contaminated with **1**. Unfortunately, **2** does not redissolve once it precipitates (a feature

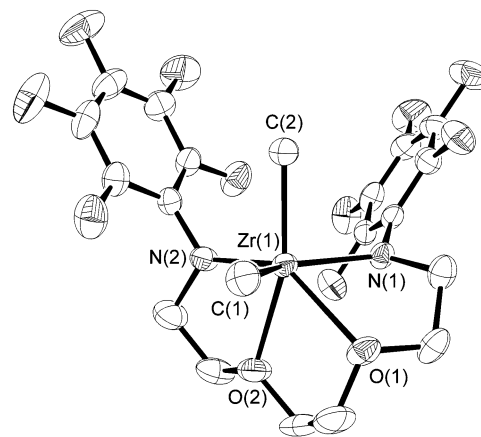
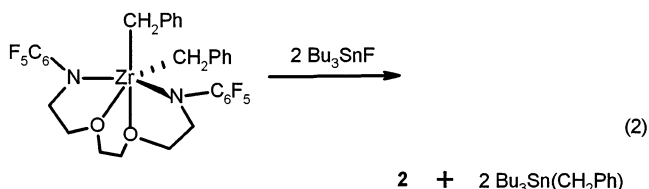


**Figure 2.** ORTEP3 drawing<sup>12</sup> (thermal ellipsoids at 30% probability) of **3**.

common to many metal fluorides due to strong bridging interactions), so we were unable to confirm the structure of this compound by X-ray diffraction.

Complex **2** can be independently prepared by the reaction of  $\text{Zr}(\text{C}_6\text{F}_5\text{NCH}_2\text{CH}_2\text{OCH}_2)_2(\text{CH}_2\text{Ph})_2$  with 2 equiv of solid  $\text{n-Bu}_3\text{SnF}$  in toluene (eq 2). Resonances due to **2** were observed in the  $^1\text{H}$  and  $^{19}\text{F}$  NMR of the supernatant after stirring overnight. In addition,  $\text{n-Bu}_3\text{Sn}(\text{CH}_2\text{Ph})$  was identified as the major soluble product by  $^1\text{H}$  NMR of the supernatant. However, the low solubility of both **2** and  $\text{n-Bu}_3\text{SnF}$  made it impossible to obtain pure **2** by this route.



To compare the behavior of various zirconium alkyls, we decided to synthesize the methyl complex  $\text{Zr}(\text{C}_6\text{F}_5\text{NCH}_2\text{CH}_2\text{OCH}_2)_2\text{Me}_2$  (**3**). The synthesis proceeded straightforwardly according to eq 3 starting from  $\text{Zr}(\text{C}_6\text{F}_5\text{NCH}_2\text{CH}_2\text{OCH}_2)_2\text{Cl}_2$  and  $\text{MeLi}$  (2 equiv). The structure of **3** was determined by X-ray crystallography; an ORTEP3 drawing is shown in Figure 2. Data collection parameters are given in Table 1, and selected bond distances and angles are collected in Table 3. Complex **3** adopts a distorted octahedral geometry with cis amido nitrogens and cis dialkyls, similar to other

(17) Typical Zr–phenyl bond lengths may be found in the following references: (a) Amor, F.; Butt, A.; du Plooy, K. E.; Spaniol, T. P.; Okuda, J. *Organometallics* **1998**, *17*, 5836. (b) Erker, G.; Czisch, P.; Mynott, R.; Tsay, H.; Kruger, C. *Organometallics* **1985**, *4*, 1310. (c) Alcock, N. W.; Clase, H. J.; Duncalf, D. J.; Hart, S. L.; McCamley, A.; McCormack, P. J.; Taylor, P. C. *J. Organomet. Chem.* **2000**, *605*, 45. (d) Kraft, B. M.; Lachicotte, R. J.; Jones, W. D. *J. Am. Chem. Soc.* **2001**, *123*, 10973. (e) Schöck, L. E.; Brock, C. P.; Marks, T. J. *Organometallics* **1987**, *6*, 232. (f) Fryzuk, M. D.; Mylvaganam, M.; Zaworotko, M. J.; MacGillivray, L. R. *J. Am. Chem. Soc.* **1993**, *115*, 10360. (g) Clegg, W.; Horsburgh, L.; Lindsay, D. M.; Mulvey, R. E. *Acta Crystallogr. C* **1998**, *C54*, 315. (h) Giannini, L.; Caselli, A.; Solari, E.; Floriani, C.; Chiesi-Villa, A.; Rizzoli, C.; Re, N.; Sgamellotti, A. *J. Am. Chem. Soc.* **1997**, *119*, 9198. (i) Scott, M. J.; Lippard, S. J. *Organometallics* **1997**, *16*, 5857. (j) Jeffrey, J.; Lappert, M. F.; Luong-Thi, N. T.; Atwood, J. L.; Hunter, W. E. *J. Chem. Soc., Chem. Commun.* **1978**, 1081. (k) Fryzuk, M. D.; Haddad, T. S.; Rettig, S. J. *Organometallics* **1989**, *8*, 1723. (l) Yue, N.; Hollink, E.; Guerin, F.; Stephan, D. W. *Organometallics* **2001**, *20*, 4424. (m) Lee, H.; Bridgewater, B. M.; Parkin, G. *J. Chem. Soc., Dalton Trans.* **2000**, 4490.

(18)  $^{19}\text{F}$  NMR chemical shifts for perfluorinated aryl groups range from -110 to -180 ppm ( $\delta$  relative to  $\text{CCl}_3\text{F}$ ): (a) Mann, B. E. In *NMR of the Periodic Table*; Harris, R. K., Mann, B. E., Eds.; Academic Press: London, 1978. (b) Jameson, C. J. In *Multinuclear NMR*; Mason, J., Ed.; Plenum Press: New York, 1987.

(19)  $^{19}\text{F}$  NMR chemical shifts for series of cyclopentadienyl zirconium complexes containing terminal Zr–F groups range from +20 to +110 ppm ( $\delta$  relative to  $\text{CCl}_3\text{F}$ ): (a) Shah, S. A. A.; Dorn, H.; Voigt, A.; Roesky, H. W.; Parisini, E.; Schmidt, H.; Noltemeyer, M. *Organometallics* **1996**, *15*, 3176. (b) Shah, S. A. A.; Dorn, H.; Roesky, H. W.; Parisini, E.; Schmidt, H.; Noltemeyer, M. *J. Chem. Soc., Dalton Trans.* **1996**, 4143. (c) Shah, S. A. A.; Dorn, H.; Gindl, J.; Noltemeyer, M.; Schmidt, H.; Roesky, H. W. *J. Organomet. Chem.* **1998**, *550*, 1. (d) Herzog, A.; Liu, F.; Roesky, H. W.; Demsar, A.; Keller, K.; Noltemeyer, M.; Pauer, F. *Organometallics* **1994**, *13*, 1251. (e) Murphy, E. F.; Lubben, T.; Herzog, A.; Roesky, H. W.; Demsar, A.; Noltemeyer, M.; Schmidt, H. *Inorg. Chem.* **1996**, *35*, 23. (f) Herzog, A.; Roesky, H. W.; Jager, F.; Steiner, A. *J. Chem. Soc., Chem. Commun.* **1996**, 29. (g) Kraft, B. M.; Lachlotte, R. J.; Jones, W. D. *Organometallics* **2002**, *21*, 727.

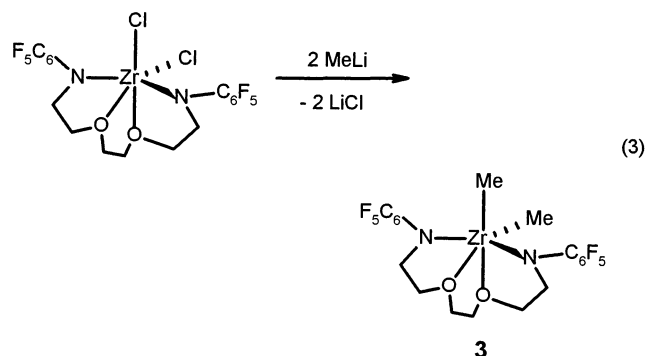
(20)  $^{19}\text{F}$  NMR chemical shifts for series of cyclopentadienyl zirconium complexes containing bridging Zr–F groups range from -19 to -112 ppm ( $\delta$  relative to  $\text{CCl}_3\text{F}$ ): Please see ref 19c–f and: Chen, Y.; Metz, M. V.; Li, L.; Stern, C. L.; Marks, T. J. *J. Am. Chem. Soc.* **1998**, *120*, 6287.



**Table 3.** Selected Bond Distances (Å) and Angles (deg) for **3**

Bond Distances			
Zr(1)–N(1)	2.133(3)	Zr(1)–N(2)	2.103(3)
Zr(1)–O(1)	2.411(2)	Zr(1)–O(2)	2.296(2)
Zr(1)–C(1)	2.256(3)	Zr(1)–C(2)	2.251(3)
Bond Angles			
N(1)–Zr(1)–N(2)	116.66(10)	N(1)–Zr(1)–O(1)	69.05(9)
N(1)–Zr(1)–O(2)	101.74(10)	N(1)–Zr(1)–C(1)	133.56(13)
N(1)–Zr(1)–C(2)	87.34(12)	N(2)–Zr(1)–O(1)	139.54(10)
N(2)–Zr(1)–O(2)	70.82(10)	N(2)–Zr(1)–C(1)	109.73(13)
N(2)–Zr(1)–C(2)	89.48(12)	O(1)–Zr(1)–O(2)	68.88(10)
O(1)–Zr(1)–C(1)	77.59(11)	O(1)–Zr(1)–C(2)	130.81(12)
O(2)–Zr(1)–C(1)	95.05(12)	O(2)–Zr(1)–C(2)	160.30(12)
C(1)–Zr(1)–C(2)	91.03(13)	Zr(1)–N(1)–C(3)	115.7(2)
Zr(1)–N(1)–C(15)	123.3(2)	C(3)–N(1)–C(15)	117.0(3)
Zr(1)–N(2)–C(8)	123.3(2)	Zr(1)–N(2)–C(9)	122.7(2)
C(8)–N(2)–C(9)	112.3(3)		

zirconium complexes of this ligand that we have reported.<sup>9</sup> As in earlier structures, one of the oxygen atoms (O1) is considerably further from the metal than the other, reflecting a distortion toward a five-coordinate geometry (Zr(1)–O(1) 2.411(2) Å, Zr(1)–O(2) 2.296(2) Å). The extent of this distortion is less in **3** than in previous structures, most likely due to the smaller methyl groups present here. Other metrical parameters are similar to previous structures in this family.<sup>9</sup>

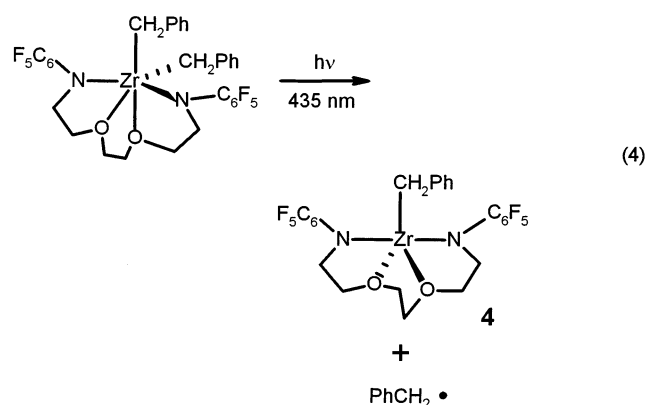


Photolysis of a colorless solution of **3** using a 435 nm filter resulted in no detectable reaction over a period of 14 h. Photolysis at a shorter wavelength (375 nm) resulted in photochemical decomposition similar to that observed for the dibenzyl complex, although the rate of decomposition was slower for **3**. A UV/vis spectrum of **3** showed no significant absorption in the visible region.

### Discussion

The pathway for the formation of **1** in the presence of light is an interesting question. Since bibenzyl is observed as a byproduct in this reaction and benzyl fluoride is not, simple abstraction of an *ortho* aryl fluorine to afford the monomer of **1** directly can be ruled out. Bibenzyl could arise either by direct reductive elimination to afford a Zr(II) species or by homolytic Zr–C bond cleavage to afford a benzyl radical and a Zr(III) benzyl complex. There have been many claims for photochemical reductive elimination to form Zr(II) in the literature, mostly for Cp<sub>2</sub>ZrR<sub>2</sub> complexes.<sup>2</sup> However, in most instances reductive elimination was assumed to occur based on the observation of R–R products, and few mechanistic studies supporting this idea have been presented.<sup>21,22</sup> On the other hand, in

recent years there have been a number of photochemical studies on Cp<sub>2</sub>ZrR<sub>2</sub> and related complexes that clearly show the formation of both Zr(III) and the free organic radicals by EPR spectroscopy.<sup>3,23</sup> Indeed, in many cases the Zr(III) species are stable enough to isolate<sup>24</sup> from the reaction mixture, although they are often prone to subsequent thermal disproportionation to Zr(II) and Zr(IV).<sup>3i</sup> A broad and weak EPR signal (*g* = 2.001) was observed during the photolysis of Zr(C<sub>6</sub>F<sub>5</sub>NCH<sub>2</sub>CH<sub>2</sub>OCH<sub>2</sub>)<sub>2</sub>(CH<sub>2</sub>Ph)<sub>2</sub>, providing some support for initial formation of a benzyl radical and a Zr(III) benzyl species **4** (eq 4).<sup>25</sup> The energy available from 435 nm light (276 kJ mol<sup>−1</sup>) is similar to the measured strength of Zr–benzyl carbon bonds (263 kJ mol<sup>−1</sup>),<sup>26</sup> lending further support to homolytic Zr–C bond cleavage as the initial photochemical reaction. The lack of reaction for **3** is probably due to the lack of absorption in the visible spectrum<sup>27</sup> and the greater bond strength of Zr–Me bonds (285 kJ mol<sup>−1</sup>).<sup>26</sup>



Assuming that photolysis initially produces **4**, the question still remains as to how **4** converts to the

(21) There is more convincing evidence for ligand-induced thermal reductive elimination from Zr(IV) dialkyls: (a) Gell, K. I.; Harris, T. V.; Schwartz, J. *Inorg. Chem.* **1981**, *20*, 481. (b) Gell, K. I.; Schwartz, J. *J. Am. Chem. Soc.* **1981**, *103*, 2687. (c) Yoshifuji, M.; Gell, K. I.; Schwartz, J. *J. Organomet. Chem.* **1978**, *153*, C15. (d) Gell, K. I.; Schwartz, J. *J. Organomet. Chem.* **1978**, *162*, C11. (e) Gell, K. I.; Schwartz, J. *J. Chem. Soc., Chem. Commun.* **1979**, 244.

(22) Some evidence for photochemical reductive elimination from Cp<sub>2</sub>Zr(R)(H) type compounds (Cp = C<sub>5</sub>Me<sub>5</sub>, R = Ph and CH<sub>2</sub>CH(CH<sub>3</sub>)<sub>2</sub>; Cp = C<sub>5</sub>H<sub>5</sub>, R = CH<sub>2</sub>PPh<sub>2</sub>) has been presented, although the possible involvement of radical pathways was not investigated: (a) Miller, F. D.; Sanner, R. D. *Organometallics* **1988**, *7*, 818. (b) Raoult, Y.; Choukroun, R.; Blandy, C. *Organometallics* **1992**, *11*, 2443.

(23) Bonomo, L.; Toraman, G.; Solari, E.; Scopelliti, R.; Floriani, C. *Organometallics* **1999**, *18*, 5198.

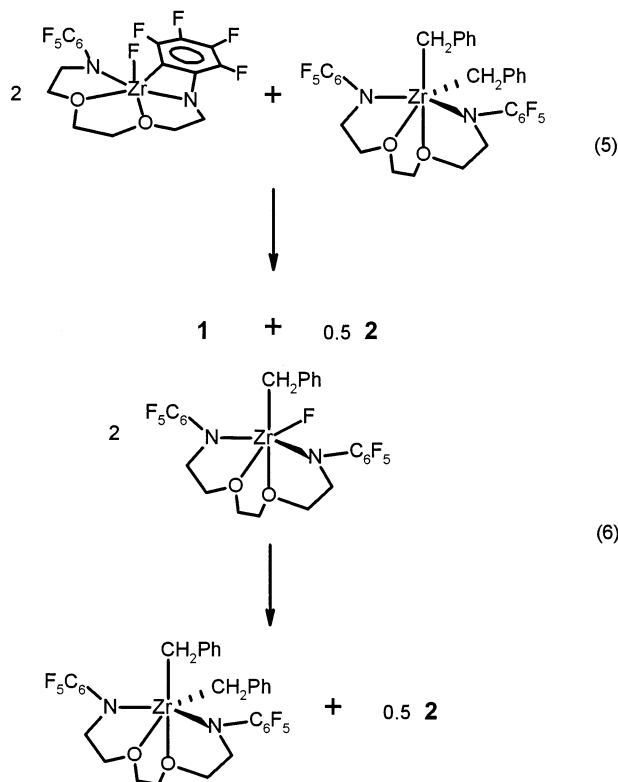
(24) (a) Williams, G. M.; Schwartz, J. *J. Am. Chem. Soc.* **1982**, *104*, 1122. (b) Samuel, E. *Inorg. Chem.* **1983**, *22*, 2967. (c) Atkinson, J. M.; Brindley, P. B.; Davies, A. G.; Hawari, J. A. *J. Organomet. Chem.* **1984**, *264*, 253. (d) Choukroun, R.; Gervais, D. *J. Chem. Soc., Chem. Commun.* **1985**, 224. (e) Samuel, E.; Guery, D.; Vedel, J.; Basile, F. *Organometallics* **1985**, *4*, 1073. (f) Choukroun, R.; Basso-Bert, M.; Gervais, D. *J. Chem. Soc., Chem. Commun.* **1986**, 1317. (g) Blandy, C.; Locke, S. A.; Young, S. J.; Shore, N. E. *J. Am. Chem. Soc.* **1988**, *110*, 7540. (h) Choukroun, R.; Gervais, D.; Raoult, Y. *Polyhedron* **1989**, *8*, 1758. (i) Fryzuk, M. D.; Mylvaganam, M.; Zaworotko, M. J.; MacGillivray, L. R. *Polyhedron* **1996**, *15*, 689.

(25) Given the long photolysis time required to convert all of the starting material (as monitored by NMR), the steady state concentration of benzyl radicals is likely to be very low, making observation difficult.

(26) Some pertinent group 4 metal–carbon bond dissociation enthalpies (kJ mol<sup>−1</sup>) from ref 6b: Zr–CH<sub>2</sub>Ph 263 (Zr(CH<sub>2</sub>Ph)<sub>4</sub>); Zr–Me 285 (Cp<sub>2</sub>ZrMe<sub>2</sub>), 284 (Cp<sub>2</sub><sup>+</sup>ZrMe<sub>2</sub>); Ti–CH<sub>2</sub>Ph 237 (Cp<sub>2</sub>Ti(CH<sub>2</sub>Ph)<sub>2</sub>); Ti–Me 298 (Cp<sub>2</sub>TiMe<sub>2</sub>).

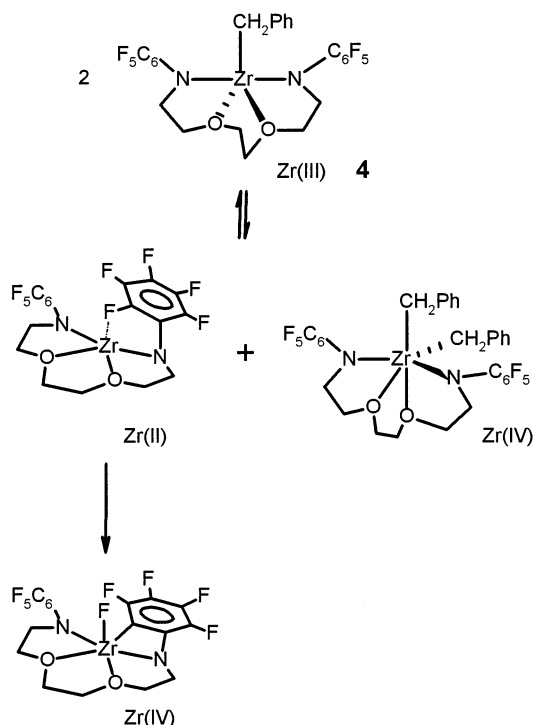
(27) The benzyl complex Zr(C<sub>6</sub>F<sub>5</sub>NCH<sub>2</sub>CH<sub>2</sub>OCH<sub>2</sub>)<sub>2</sub>(CH<sub>2</sub>Ph)<sub>2</sub> shows a shoulder at 259 nm with an  $\epsilon$  value of 70 700 M<sup>−1</sup> cm<sup>−1</sup>. Unlike the methyl derivative, this absorption tails significantly into the visible region, resulting in the yellow color of the complex.

observed products **1** and **2**. Two distinctly different routes can be envisioned: (a) disproportionation of Zr(III) complex **4** into Zr(IV) and Zr(II) species followed by oxidative addition of an *ortho* aryl C–F bond (Scheme 1) or (b) electron transfer to the electron-poor C<sub>6</sub>F<sub>5</sub> ring followed by C–F bond cleavage (Scheme 2).<sup>28</sup> Both of these processes also require a ligand redistribution reaction (eqs 5, 6) in order to account for the observed products. Redistributions such as those shown in eqs 5 and 6 are very well known in zirconium chemistry. It should also be pointed out that equivalent transformations within a dimer or higher oligomeric structure can also be proposed that would account for these transformations equally well.

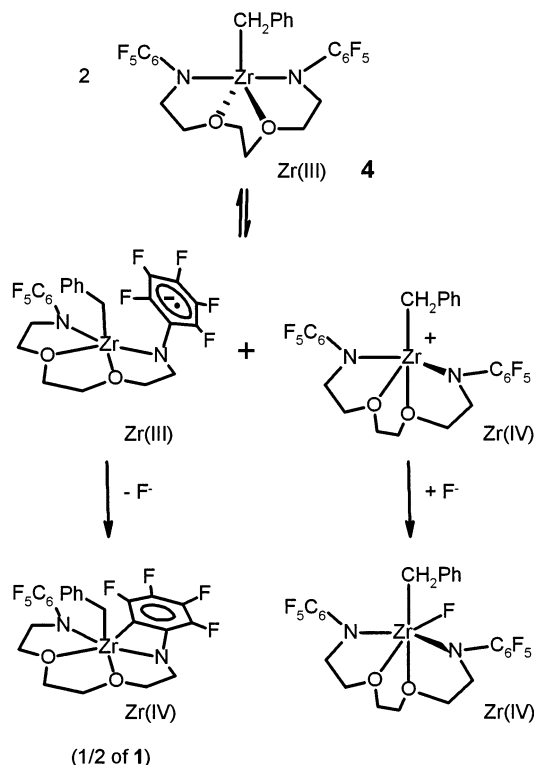


At this point, we have no evidence to distinguish between the pathways shown in Schemes 1 and 2. There is ample precedence for disproportionation of Zr(III) species into Zr(II) and Zr(IV) under thermal conditions,<sup>31</sup> and while there is no precedent for oxidative addition of an aryl C–F bond to Zr(II) that we are aware of, there are many examples with low-valent metals of later transition metal triads.<sup>5</sup> Electron transfer processes similar to that shown in Scheme 2 have been proposed to account for C–F bond activation reactions by divalent

Scheme 1



Scheme 2



(28) Important fundamental studies of the thermal C–F bond cleavage mechanism for both alkyl and aryl C–F bonds in Cp<sub>2</sub>Zr(X)<sub>2</sub> systems (X = H, C<sub>6</sub>F<sub>5</sub>) have been reported by Jones et al. These studies suggest that alkyl C–F bond cleavage proceeds by a radical pathway,<sup>28b,c</sup> while aryl C–F cleavage can occur either by radical processes<sup>28a</sup> or via formation of tetrafluorobenzene.<sup>19g,28c</sup> In the present work, it is possible to postulate a mechanism involving formation of tetrafluorobenzene and a zirconium imide that subsequently react to form the metalated C<sub>6</sub>F<sub>4</sub> unit. However, this seems unlikely to us as it necessitates C–N bond cleavage and the formation of two high-energy intermediates. (a) Edlebach, B. L.; Kraft, B. M.; Jones, W. D. *J. Am. Chem. Soc.* **1999**, *121*, 10327. (b) Kraft, B. M.; Lachicotte, R. J.; Jones, W. D. *J. Am. Chem. Soc.* **2000**, *122*, 8559. (c) Kraft, B. M.; Lachicotte, R. J.; Jones, W. D. *J. Am. Chem. Soc.* **2001**, *123*, 10973.

lanthanides with both aryl and aliphatic fluorocarbons.<sup>8</sup> Interestingly, C–F bond activation by divalent lanthanides was found to be strongly solvent dependent, proceeding at much slower rates in coordinating solvents. This was attributed to the necessity for coordination of the C–F bond to the metal center prior to electron transfer. In our experiments, we found that **1** did not form at all in THF-*d*<sub>8</sub> solution, so it is tempting to speculate that C–F coordination is also required here. Of course, it is also possible that a coordinating solvent

may have an effect on the disproportion of Zr(III) and on C–F oxidative addition, so this fact alone does not provide any distinction between the pathways in Schemes 1 and 2.

Attempts to trap a putative Zr(II) species by carrying out the photolysis reaction in the presence of alkynes or phosphines failed: **1**, **2**, and bibenzyl were obtained. Photolysis of  $\text{Zr}(\text{C}_6\text{F}_5\text{NCH}_2\text{CH}_2\text{OCH}_2)_2(\text{CH}_2\text{Ph})_2$  in a 5:1 benzene- $d_6$ – $\text{C}_6\text{F}_6$  mixture at 435 nm did not result in any evidence for intermolecular aryl C–F activation. It would appear that whatever mechanism is

operative, intramolecular C–F activation is strongly preferred.

**Acknowledgment.** The support of the Natural Sciences and Engineering Research Council of Canada is gratefully acknowledged.

**Supporting Information Available:** Tables of atomic coordinates, bond distances and angles, and anisotropic thermal parameters for **1** and **3**. This material is available free of charge via the Internet at <http://pubs.acs.org>.

OM0204181